Nonlinear Fracture Properties from Size Effect Tests

By Zdeněk P. Bažant,[1] F. ASCE, Jin-Keun Kim,[2] and Phillip A. Pfeiffer[3]

Abstract: The previously derived size effect law for blunt fracture is exploited for determining the parameters of the R-curve, of the crack band model, and of Hillerborg's fictitious crack model. No measurements of the crack length or of the unloading compliance are needed. It suffices to measure only the maximum load values for a set of geometrically similar specimens of different sizes. The parameters of the size effect law can then be identified by linear regression. The inverse slope of the regression line yields the fracture energy. The regression also has a twofold benefit: it smoothes statistically scattered data, and it extends the range of the data, so that one can do with fewer tests. From the experimentally calibrated size effect law, the R-curve may then be obtained as the envelope of the family of fracture equilibrium curves for different specimen sizes. A simple algebraic formula for this envelope is presented. The size effect regression plot makes it also possible to determine crack band model parameters, particularly the fracture energy, the crack band width, and the strain-softening modulus. The same is made possible for Hillerborg's model.

Introduction

The fracture properties of the materials in which the crack front is blunted by microcracking or yielding are not completely described by a single parameter, the fracture energy. At least two further parameters, e.g., the strength and a characteristic length, are required. Several mathematical models with additional parameters have been recently formulated (3,4,7,10,13,18,23) and shown capable of closely representing the available experimental evidence. Determination of their fracture parameters, however, is a problem. This problem will be addressed in what follows.

The simplest, although crudest, method consists of an approximate linearly elastic fracture analysis using some equivalent crack length and the R-curve, describing how the energy resistance to crack growth depends on the crack length. Irwin and Krafft et al. (14,16) proposed that the R-curve may be considered to be approximately unique. Shah and coworkers (21,22) introduced the R-curve concept to concrete. The R-curve is usually determined on a single specimen from the crack lengths observed at various load values, or on a series of specimens from their critical load values and the corresponding critical crack lengths. However, the need to measure the crack length is a considerable obstacle for a material like concrete. The crack length is hard to define since the crack tip is blurred by a microcracking zone, and even if one succeeds to locate the crack tip, its meaning is of dubious significance since the R-curve is actually a function of a certain equivalent crack length which yields the correct remote elastic stress field, rather than of the actual crack length. To avoid these difficulties, it has been attempted to determine the crack length indirectly, by measuring the specimen's compliance, either at unloading or at reloading. But this is also questionable because at unloading or reloading the microcracks within the fracture process zone do not completely close, causing the compliance for unloading and reloading to be smaller than the compliance for continued loading, which, however, cannot be measured since the crack growth cannot be arrested.

The R-curve is a device to make possible an approximate linearly elastic solution (7). A nonlinear finite element solution, which is more realistic, may be obtained with the blunt crack band model (3,9,10) in which a suitable triaxial tensile strain-softening constitutive relation is used and the crack band front is assumed to have a certain characteristic width that is a material property. Equivalent results can be obtained with Hillerborg's model (13,18), based on a softening stress-displacement relation. Following an idea suggested in Ref. 3, it will be shown that the material parameters for these models may be easily determined from the size effect.

[1]Prof. of Civ. Engrg. and Dir., Center for Concrete and Geomaterials, Northwestern Univ., Evanston, IL 60201.

[2]Asst. Prof., Korea Advanced Inst. of Sci. and Tech., Seoul; formerly Grad. Research Asst., Northwestern Univ.

[3]Resident Student Assoc. at Argonne National Laboratory; formerly Grad. Research Asst., Northwestern Univ.

Note.—Discussion open until July 1, 1986. To extend the closing date one month, a written request must be filed with the ASCE Manager of Journals. The manuscript for this paper was submitted for review and possible publication on June 15, 1984. This paper is part of the ***Journal of Structural Engineering***, Vol. 112, No. 2, February, 1986. ©ASCE, ISSN 0733-9445/86/0002-0289/$01.00. Paper No. 20394.

Size Effect Law

For blunt fracture one can generally introduce the hypothesis (5,9) that the total potential energy release W caused by fracture in a given structure depends on both: (1) The length a of the fracture; and (2) the area traversed by the fracture process zone, such that the size of the fracture process zone at failure is constant, independent of the size of the structure. Dimensional analysis and similitude arguments then show that, for geometrically similar specimens or structures made of the same material (5,6)

$$\sigma_N = Bf'_t\left(1 + \frac{d}{d_0}\right)^{-1/2} \quad \text{(1)}$$

in which $\sigma_N = P/bd$ = nominal stress at maximum load P; b = thickness; d = characteristic dimension of the structure (e.g., beam's depth); f'_t = direct tensile strength; $d_0 = \lambda_0 d_a$; d_a = aggregate size; and B, λ_0, d_0 = empirical constants. See the graph in Fig. 1. The values of B and λ_0 depend on the geometrical shape of the structure.

If the structure is very small, then $d/d_0 << 1$, and so $\sigma_N \sim Bf'_t$. This is the strength (or yield) criterion, represented by a horizontal line in Fig. 1(*a*). If the structure is very large, then $d/d_a >> 1$, and so $\sigma_N \sim \text{const.}/\sqrt{d}$. This is the size effect typical of linear elastic fracture mechanics which corresponds to the inclined straight line in Fig. 1(*a*), having the slope $-1/2$. The size effect law according to Eq. 1 represents a gradual transition from the strength (or yield) criterion to the energy criterion of linear elastic fracture mechanics. This law is only approxi-

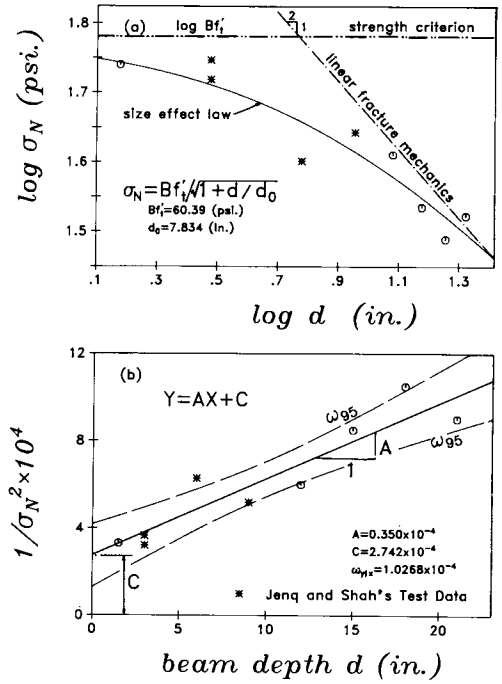

FIG. 1.—Size Effect Law and Regression Analysis of Maximum Load Data

mate because the hypothesis of a constant size of the fracture process zone at failure is not exact.

Equivalent Linear Fracture Analysis and R-Curves

Frequently, the fracture process zone is small compared to the structure dimensions and the remote stress and strain fields are almost the same as the elastic ones. The fracture may then be approximately treated as an equivalent line crack that produces the same remote elastic stress and strain fields. For this equivalent crack, the energy, R, required for crack growth (also called the fracture resistance) must be considered as a function of the crack extension c from the notch or smooth surface, i.e., $R = R(c)$ in which $c = a - a_0$; a_0 = length of the notch; and a = total length of the crack plus notch (Fig. 2). The energy that must be supplied to produce the crack is $U = b\int R(c)da - W(a)$ where $W(a)$ = the total release of strain energy from the structure. An equilibrium state of fracture occurs if $\delta U = 0$. Since $\delta U = (\partial U/\partial a)\delta a = 0$, in which $\partial U/\partial a = b(R - G) = 0$, and $bG = W' = \partial W/\partial a$, it follows that fracture equilibrium takes place if $G(a) = R(c)$, in which G is the energy release rate of the structure. The equilibrium fracture state is stable if $\partial^2 U$ is positive definite. Since $\delta^2 U = (\partial^2 U/\partial a^2)\delta a^2$ where $\partial^2 U/\partial a^2 = b[dR/dc - \partial G(a)/\partial a] = B[R'(c) - G'(a)]$ and $bG'(a) = W''(a) = \partial^2 W/\partial a^2$, the following conditions ensue:

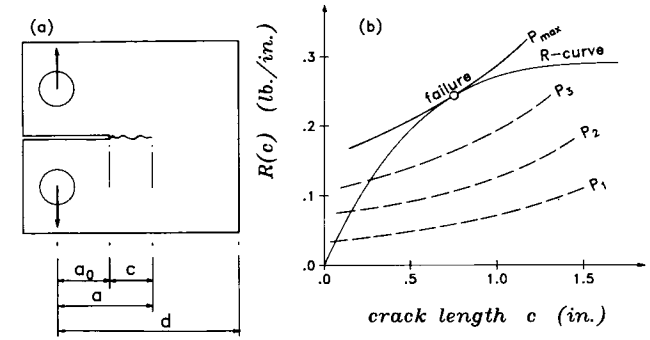

FIG. 2.—R-Curve

$$R'(c) - G'(a) > 0 \quad \text{(stable)}; \qquad R'(c) - G'(a) = 0 \quad \text{(critical)} \ldots\ldots\ldots (2)$$

Considering structures that are geometrically similar but could have dissimilar notches, and using dimensional analysis, one can show that

$$G(a) = \frac{W'(a)}{b} = \frac{P^2 g(\alpha)}{E_c b^2 d} \ldots\ldots\ldots (3a)$$

$$G'(a) = \frac{W''(a)}{b} = \frac{P^2 g'(a)}{E_c b^2 d^2} \ldots\ldots\ldots (3b)$$

in which $\alpha = a/d = (a_0 + c)/d$; $g'(\alpha) = dg(\alpha)/d\alpha$; E_c = Young's elastic modulus; and $g(\alpha)$ = nondimensional function which characterizes the geometry of the structure and can be determined by linear finite element analysis or found for typical shapes in handbooks (19) ($G = K_I^2/E_c$, K_I = stress intensity factor). Substitution of Eqs. 3*a*–*b* into Eq. 2 leads to the conditions

$$R(c)\,g'(\alpha) - R'(c)\,g(\alpha)\,d > 0 \quad \text{(stable)};$$

$$R(c)\,g'(\alpha) - R'(c)\,g(\alpha)\,d = 0 \quad \text{(critical)} \ldots\ldots\ldots (4)$$

Alternatively, since $dg/dc = dg/da = g'(\alpha)/d$, this is equivalent to $R(c)/g(\alpha)$ = max. Thus, one may simply try many values of c and identify which one yields the maximum.

The R-curve concept rests on the hypothesis (14,16) that function $R(c)$ may be approximately considered to be a unique material property. Keep in mind, though, that function $R(c)$ is generally not exactly the same for different specimen shapes and different notch lengths.

Identification of Fracture Energy from Size Effect

As an example, consider three-point bent fracture tests on specimens of various depths d, all with thickness b = 1 in., span to depth ratio L/d = 4, and initial notch depth $a_0 = d/3$; also, $E_c = 4.3 \times 10^6$ psi and f_c' = 3,650 psi (15). According to Tada (19), $g(\alpha) = 16\pi\,\alpha(1.635 - 2.603\,\alpha$

$+ 12.30\ \alpha^2 - 21.27\ \alpha^3 + 21.86\ \alpha^4)^2$. The following experimental data are considered:

$$\left.\begin{array}{l} d = 1.5, \quad 3^*, \quad 6^*, \quad 9^*, \quad 12, \quad 15, \quad 18, \quad 21 \text{ in.}; \\ P = 82.4, \ 156.9^* \text{ and } 167.4^*, \ 239.6^*, \ 395.6^*, \ 490.0, \ 514.5, \ 555.5, \ 700 \text{ lbs} \end{array}\right\} \quad (5)$$

(asterisks label the values taken from Jenq and Shah's measurements, Ref. 15). The inevitable statistical scatter may be smoothed out using the size effect law in Eq. 1. This equation may be algebraically transformed to a linear form, $Y = AX + C$, in which $X = d$; $Y = \sigma_N^{-2} = b^2d^2/P^2$; $A = C/d_0$; and $C = 1/(B^2 f_t'^2)$. Thus, coefficients A and C can be determined by linear regression, either by computer or by hand; see Fig. 1(*b*). This yields $C = 2.742 \times 10^{-4}$, and $A = 0.350 \times 10^{-4}$. The coefficient of variation ω of the vertical deviations from the regression line and the corresponding 95% confidence limits are also shown in Fig. 1(*b*).

As mentioned before, in the limiting case of very large sizes ($d/d_0 >> 1$) linear elastic fracture mechanics applies. We call the corresponding limit value of R the fracture energy G_f. It may be obtained from the inclined asymptote in Fig. 1(*a*), i.e., from Eq. 1 when 1 is neglected, in which case $Y = AX = \sigma_N^{-2}$. Noting that $\alpha \rightarrow \alpha_0$ for failure of very large specimens, and substituting $X = d$ and $\sigma_N^2 = G_f E_c / g(\alpha_0) d$, which follows from Eq. 3*a* by setting $G = G_f$ and $P = \sigma_N bd$, we obtain the result

$$G_f = \frac{g(\alpha_0)}{AE_c} \quad \ldots\ldots (6)$$

in which $\alpha_0 = a_0/d$. So the fracture energy is inversely proportional to the slope, A, of the size effect regression line. Note that Eq. 6 does not depend on the hypothesis that the R-curve is unique.

Substituting A and $g(\alpha_0) = 43.76$ from function $g(\alpha)$, Eq. 6 yields $G_f = 0.291$ lb/in. This may be compared to the value obtained by Jenq and Shah (15) from their measurements not involving the size effect; it was 0.42 lb/in. This is not too close to our value, however, their method of measurement lends their G_f value a somewhat different physical meaning.

Evaluating $Y = AX + C$ for various values of d, we may further obtain smoothed maximum load data P:

$$\left.\begin{array}{l} d = 1.5, \quad 3, \quad 6, \quad 9, \quad 12, \quad 15, \quad 18, \quad 21 \text{ in.}; \\ P = 83.0, \ 154.1, \ 272.7, \ 370.8, \ 455.4, \ 530.6, \ 598.6, \ 661.0 \text{ lbs} \end{array}\right\} \quad \ldots\ldots (7)$$

(this same smoothed data would be obtained even if the measurements included only the three asterisk-marked values in Eq. 5).

Geometric similarity is required only in two dimensions, and thus the specimens could have different thicknesses b. However, the fracture energy is not constant along the front edge of crack, and thus the thickness has some effect on the mean G_f for the whole thickness. There are two sources of the thickness effect. One is the disturbance of the free surface boundary conditions due to Poisson effect and surface point singularity of elastic solution (8), and another one is the different influence of the aggregate size near the surface and the interior on the microcracking zone size. The former effect is eliminated if b/d is constant, and the latter one if b is constant. Thus, no perfect answer exists for the choice of thickness. The condition b = constant seems, nevertheless, more important.

The fact that the size effect plot [Fig. 1(*a*)] possesses an inclined asymptote implies that the R-curve must have a horizontal asymptote, a property previously sometimes regarded as uncertain. The fracture energy, G_f, a term reserved here strictly for the final asymptotic value of R, is uniquely defined by this asymptote. Thus, the value of the fracture energy as defined here must be considered size-independent. Compared to other definitions of G_f the present one is most relevant for determining the failure loads at different structure sizes.

If the three-point bent fracture specimen is sufficiently slender, i.e., L/d is sufficiently large, the failure is governed primarily by the bending moment M in the notched cross section, and the effect of the shear force may be neglected. Then it is not necessary for the specimens of different sizes to be geometrically similar. It suffices if the notched cross sections are similar, i.e., have the same ratios a_0/d. Let the reference specimen be characterized by $d = d_1$ and $L = L_1$. Then the maximum load P_2 measured for a dissimilar specimen of dimensions L_2, d_2 such that $L_2/d_2 \neq L_1/d_1$ must be transformed to the maximum load P_2^* corresponding to span $L_2^* = L_1 d_2/d_1$. Equating the bending moments, $(1/4)\ P_2 L_2 = (1/4)\ P_2^*(L_1 d_2/d_1)$, we obtain

$$P_2^* = P_2 \frac{L_2 d_1}{L_1 d_2} \quad \ldots\ldots (8)$$

This value, rather than the measured load P_2, must then be used in the size effect regression plot [Fig. 1(*b*)].

If the beam is not very slender, a correction for the dependence of $g(\alpha)$ on L/d should be introduced. The similar specimen of span L_2^* and the actual, dissimilar specimen of span L_2 have the same cross section, and therefore they may be assumed to fail at the same crack length c, i.e., at the same a or the same α ($\alpha = a/d$). Thus, the energy release rates G at maximum load must be the same for both specimens, and so (according to Eq. 3*a*) $G = P_2^2 g(\alpha_2)/E_c b^2 d_2^2 = P_2^{*2}\ g^*(\alpha_2)/E_c b^2 d_2^2$ where $\alpha_2 = a_2/d_2 = a_2^*/d_2$; this yields

$$P_2^* = P_2 \sqrt{\frac{g(\alpha_2)}{g^*(\alpha_2)}} \quad \ldots\ldots (9)$$

It may be checked numerically that if both L_2/d_2 and L_2^*/d_2 are large, Eq. 9 is reduced to Eq. 8.

Eq. 9 has an inconvenient feature in that the crack length c at failure must be estimated before P_2^* can be calculated; $\alpha_2 = (a_0 + c)/d_2$. The estimate, however, can be improved iteratively. For this purpose one has to solve also the R-curve as described in the next section, and then solve a_2 from Eq. 4, upon which one may obtain an improved value of P_2^* from Eq. 9.

Identification of R-Curve as an Envelope

Consider again that maximum load P for a series of geometrically similar specimens has been measured. However, the crack lengths c cor-

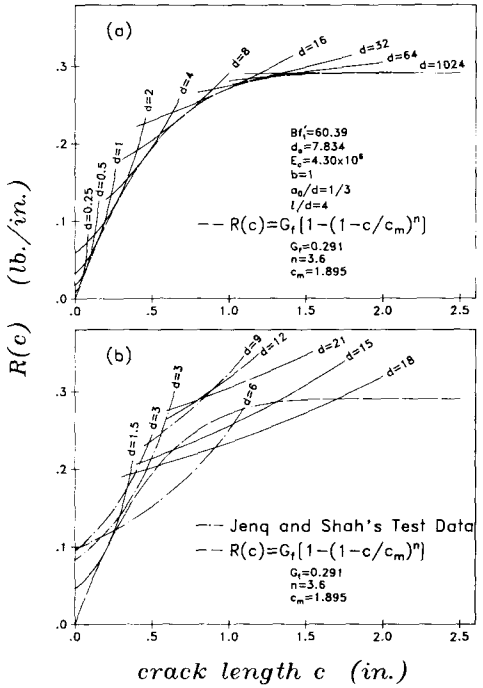

FIG. 3.—R-Curve as Envelope for: (*a*) Smoothed Data; (*b*) Unsmoothed Data

responding to each failure load are unknown. Using function $g(\alpha)$, which is common to all specimens, we can plot according to Eq. 3*a* the equilibrium curves of G versus c for each of these specimens, as shown in Fig. 3(*a*). Only one point on each of these equilibrium curves is the failure state. Now, each equilibrium curve of G versus c must contain a failure point, and so this curve should be tangent to the R-curve [Fig. 3(*a*)]. Consequently, the R-curve is the envelope of all equilibrium curves of G versus c for the failure loads of specimens of different sizes.

To prove it rigorously, the curves in Fig. 3(*a*) may be considered as a one-parameter family of curves with parameter λ, described by the equation $f(c, G, \lambda) = 0$, in which $f(c, G, \lambda) = R(c) - G(a_0 + c, \lambda)$. Differentiation of this then yields $\partial f/\partial c + G'\partial f/\partial G + (\partial f/\partial \lambda)\ \partial\lambda/\partial c = R' - G' + (\partial f/\partial\lambda)(\partial\lambda/\partial c) = 0$. The envelope of the family of all curves is given by $\partial f/\partial\lambda = 0$. This leads then to the relation $R'(c) - G' = 0$, which is the same as Eq. 2 for the critical state. So the envelope represents the critical states.

It may now seem that the R-curve could be constructed as an envelope directly from measured data (Eq. 5) by plotting G versus c according to Eq. 3*a*. In practice, however, such an approach does not work. This is because of inevitable statistical scatter of test results. One needs some simple law which could be used to smooth out the experimental data before construction of the envelope is attempted. Eq. 1 provides such a law. So we use the smoothed data from Eq. 7, and for each pair of d and P we plot the equilibrium curve of G versus c according to Eq. 3*a*.

This yields the family of curves in Fig. 3(*a*). The envelope may now be easily obtained.

Although, from the viewpoint of representation of the original measured data, many different formulas are about equally good (7) (due to large scatter of data), the choice of formulas becomes more limited if one wants to closely match the size effect law (Eq. 1). From this viewpoint, the following formula appears to work well

$$R(c) = G_f\left[1 - \left(1 - \frac{c}{c_m}\right)^n\right] \quad \text{for} \quad c \le c_m; \quad R(c) = G_f \quad \text{for} \quad c \ge c_m \ \ldots\ (10)$$

According to the values in Eq. 7 $G_f = 0.291$ lb/in., $c_m = 1.895$ in., and $n = 3.6$. As seen from Fig. 3(*a*), this formula appears to give a nearly perfect envelope. Alternatively, one can also use the formula

$$R(c) = G_f\left(1 + \frac{k_0}{c + k_1 c^n}\right)^{-m} \ \ldots\ (11)$$

with coefficients G_f, k_0, k_1, m, and n. It so happens that the approximations of the envelope remain quite good if m and n are fixed as $m = 0.19$ and $n = 4.24$. Then Eq. 11 has the advantage that parameters k_0 and k_1 may be determined by linear regression. Indeed, Eq. 11 can be transformed to the form $y = A'x + C'$, in which $x = c^{n-1}$; $y = [(G_f R^{-1})^{1/m} - 1]^{-1}/c$; $A' = k_1 C'$; $C' = 1/k_1$. For the data in Eq. 7, one obtains $k_0 = 1.53 \times 10^{10}$ and $k_1 = 3.58 \times 10^{10}$.

For comparison, let us see what we would get if the size effect law (Eq. 1) were unknown. Then, plotting the curves of G versus c on the basis of the measured maximum loads (Eq. 5), we would get the family of curves shown in Fig. 3(*b*). This family has no common envelope, and since the value of c at failure for each of the curves is unknown, it is not even possible to deduce any R-curve by statistical regression. Thus, knowledge of the size effect law (Eq. 1) is crucial for being able to determine the R-curve without having to measure the crack lengths at failure, a task notorious for its difficulty and ambiguity. For comparison, Fig. 3(*b*) also shows the R-curve which is obtained if the measured maximum loads are first smoothed with the size effect law, Eq. 1.

Instead of constructing the envelope graphically [Fig. 3(*a*)], one can define it analytically. For this purpose, we insert $P = \sigma_N bd$ in Eq. 3*a*, and we set equal to 0 the partial derivative of this equation with respect to λ at constant G, which is the condition for an envelope. This yields

$$G = \frac{d_0}{E_c}\lambda\sigma_N^2(\lambda)g(\alpha); \quad \alpha = \frac{a_0 + c}{\lambda d_0} \ \ldots\ (12)$$

$$\frac{a_0 + c}{d_0}\frac{1}{g(\alpha)}\frac{dg(\alpha)}{d\alpha} = \lambda + \frac{2\lambda^2}{\sigma_N(\lambda)}\frac{d\sigma_N(\lambda)}{d\lambda} \ \ldots\ (13)$$

These equations represent a parametric equation of the R-curve, with λ as a parameter. To calculate points on the R-curve, a series of λ values is chosen, and for each λ the value of c is solved from Eq. 13 by Newton

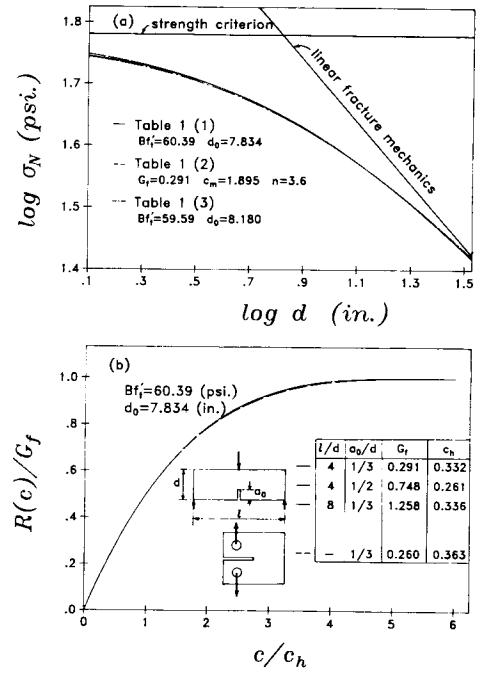

FIG. 4.—Shape of R-Curve and Corresponding Size Effect Curve

iterative method. G then results by substitution in Eq. 12 (in which $c = \alpha\lambda d_0 - a_0$).

It is interesting to recalculate the size effect curve $\sigma_N(\lambda)$ back from the curve $R(c)$ that has previously been calculated from the size effect curve according to Eq. 1. Since Eq. 10 for the R-curve is only approximate, the resulting curve $\sigma_N(\lambda)$ cannot be exactly the same as Eq. 1, but it ought to be almost the same. The calculations for the present example confirm that it is [see Fig. 4(*a*) and Table 1].

As is well known, different specimen geometries lead to different R-curves, although usually the differences are not large. To check it, we calculate the R-curves for three-point bent specimens of various span-to-depth ratios, various notch length-to-depth ratios, and also for a different type of specimen—the compact tension specimen, determining $g(\alpha)$ from Tada (19). The resulting R-curves are plotted in Fig. 4(*b*), in which they are scaled both vertically and horizontally so that the final value will be 1.0 and the point where one-half of the final value is reached will be common to all the R-curves. Note the smallness of the differences among the shapes of these R-curves; they are hardly distinguishable graphically. Therefore, the R-curves from Fig. 4(*b*) are also tabulated in Table 2; the parameters for the three columns in this table are G_f = 0.291, 0.748, 1.258, 0.260 lb/in., c_m = 1.895, 1.491, 1.919, 2.280 in., and c_h = 0.332, 0.261, 0.336, 0.363 in., respectively. We may conclude that the relationship between the size effect law and the R-curve for a given

TABLE 1.—Size Effect Curves

Depth, d (1)	Smoothed max. P data; Bf'_t = 60.39, d_0 = 7.834 (2)	After conversion to R-curve and back; c_m = 1.895, n = 3.6 (3)	After regression of Col. 2; Bf'_t = 59.59, d_0 = 8.180 (4)
0.1	60.01	59.05	59.23
0.2	59.63	58.73	58.87
0.5	58.55	57.80	57.85
1	56.87	56.33	56.25
2	53.90	53.64	53.42
5	47.18	47.22	46.95
10	40.03	40.08	39.97
20	32.04	32.02	32.11
50	22.23	22.17	22.34
100	16.28	16.24	16.39
200	11.73	11.70	11.81
500	7.50	7.49	7.56

specimen geometry may be considered as approximately unique.

In the size effect law (Eq. 1), there are two independent parameters, Bf'_t and d_0. For the relative R-curve values $R(c)/G_f$ in Eq. 10, there are also only two parameters, n and c_m (G_f is obtained by linear regression from Eq. 10). Hence, for all specimens for which the values of Bf'_t and d_0 are the same, the values of nondimensional parameters n and c_m should

TABLE 2.—Values of $R(c)/G_f$ for Curves in Fig. 4(*b*) Defining Relative Shapes of R-Curves for Different Specimen Types and the Same Size Effect Law (Eq. 1)

	Three-Point Bent			
c/c_h (1)	l/d = 4; a_0/d = 1/3, n = 3.6, c_m = 1.895, c_h = 0.332 (2)	l/d = 4, a_0/d = 1/2, n = 3.6, c_m = 1.491, c_h = 0.261 (3)	l/d = 8, a_0/d = 1/3, n = 3.6, c_m = 1.919, c_h = 0.336 (4)	Compact tension; a_0/d = 1/3, n = 4.0, c_m = 2.280, c_h = 0.363 (5)
0	0	0	0	0
0.5	0.2810	0.2810	0.2810	0.2822
1.0	0.5	0.5	0.5	0.5
1.5	0.6662	0.6662	0.6662	0.6640
2.0	0.7883	0.7883	0.7883	0.7839
2.5	0.8743	0.8743	0.8743	0.8685
3.0	0.9317	0.9317	0.9317	0.9254
3.5	0.9672	0.9672	0.9672	0.9614
4.0	0.9870	0.9870	0.9870	0.9825
4.5	0.9963	0.9963	0.9963	0.9935
5.0	0.9995	0.9995	0.9995	0.9983
5.5	1	1	1	0.9998
6.0	1	1	1	1
6.5	1	1	1	1

Specimen Type							
		2d, $2a_0$	2d, a_0	a_0, d	d, $\frac{1}{2}a_0$, l		a_0, l/3, l
					l/d=4	l/d=8	
$a_0/d=1/3$	n	2.8	2.7	4.0	3.6	3.6	3.5
	c_m/d_0	0.2930	0.3569	0.2911	0.2419	0.2450	0.2427
$a_0/d=1/2$	n	3.7	4.3	4.1	3.6	3.6	3.8
	c_m/d_0	0.3542	0.5037	0.2190	0.1903	0.1944	0.2062

FIG. 5.—Parameters of R-Curve Corresponding to Size Effect Law

also be the same. This means that all geometrically similar specimens of different sizes should be characterized by the same values of n and c_m/d_0. This property is verified by numerical examples. We may, therefore, construct a table of n and c_m/d_0 for various typical specimen geometries, see Fig. 5. For the specimen geometries in Fig. 5, it is not necessary to construct the R-curve as an envelope. It suffices to carry out the linear regression shown in Fig. 1(*b*), and then take n and c_m/d_0 from Fig. 5.

For comparison, consider now a series of tests of specimens of the same dimension d but different notch lengths a_0. The maximum loads P are measured for various a_0. If one wishes to use the envelope property, one must plot for each pair of a_0 and P the curve of G versus c

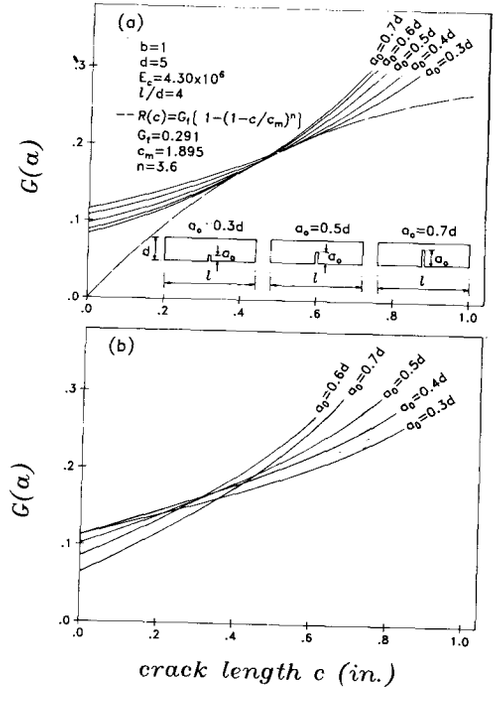

FIG. 6.—R-Curve as Envelope for Various Notch Lengths in Specimen of One Size: (*a*) Smoothed; (*b*) Unsmoothed Data

where $G = P^2(\alpha)/(E_c b^2 d)$ and $\alpha = (a_0 + c)/d$. If the measurements were perfect, then these plots would yield a family of curves such as illustrated in Fig. 6(*a*), for which the envelope representing the R-curve can be, in theory, constructed. In practice, this does not work, for two reasons: (1) If d is constant, only a small portion of the R-curve is covered by the failure states for various a_0-values [Fig. 6(*a*)]. There is always statistical scatter, which causes that these plots yield a family of curves such as illustrated in Fig. 6(*b*). Obviously, no envelope can be constructed, and thus smoothing of the data is imperative before the envelope could be traced. However, for the effect of the notch length a_0 at a constant cross section dimension d, there is no simple law which could be used for smoothing the data. A considerably more sophisticated procedure is required to determine the material parameters (7).

Determining G_f from Complete Load-Deflection Diagram.—It has been suggested that the fracture energy G_f can be determined as the area under the complete load-deflection diagram (17,18,20). However, the G_f values obtained in this manner are frequently inconsistent and scattered. One source of error is that on larger specimens, due to the specimen's own weight, the declining load-deflection diagram cannot be measured down to zero due to instability, and the tail must be estimated. Another source of error is that energy dissipation which does not produce fracture may occur in the system.

Still another source of error and a basic difference from the present approach is that the load values for all crack lengths affect the result, while here only the peak load value matters. The question then is whether the fracture process zone at other than peak load values dissipates energy at the same rate as it does at the peak load. This would certainly be true if the fracture were a straight line, with a sharp tip and a fracture process zone of negligible size. This is not so, however. It is likely that the width and the length of the microcracking zone at the fracture front are different than they are at the peak load, and the fact that G_f is far larger than double the theoretical specific surface Gibbs' free energy of the solid serves as the proof that much energy dissipation must occur

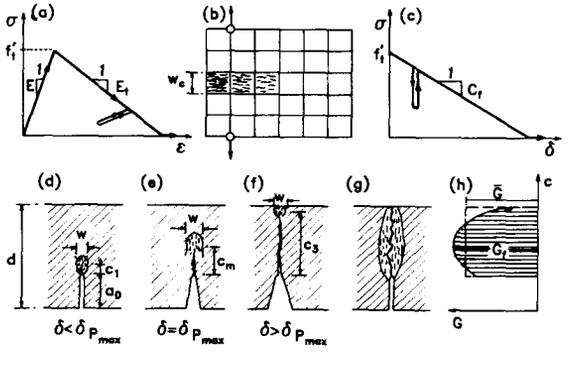

FIG. 7.—(*a*) Uniaxial Stress-Strain Relation for Crack Band Model; (*b*) Finite Element for Crack Band Model; (*c*) σ-δ Relation for Fictitious Crack Model of Hillerborg; (*d–h*) Explanation of Energy Dissipation during Crack Growth

due to microcracking on the sides of the final continuous crack. The width of the microcracking zone ahead of the fracture front is assumed to be constant in the crack band model as well as Hillerborg's fictitious crack model, but this is no doubt a simplification. In fact, it is likely that the width w of this zone varies [Fig. 7(*g*)], and especially that the widths at crack initiation [Fig. 7(*d*)] and at crack termination [Fig. 7(*f*)] may be quite different from the width at the peak load [Fig. 7(*e*)], at which the fracture front is remote from both the notch and the opposite face. Consequently, G along the crack path is variable [Fig. 7(*h*)] and the mean value $\bar{G}$ (obtained by dividing the area under the load-deflection curve by the ligament length d-a_0) need not be the same as the value of G_f at maximum load [Fig. 7(*h*)].

Now, of the values $\bar{G}$ and G_f [Fig. 7(*h*)], which one is more useful? That depends. If we need to predict the peak loads or the response near the peak loads, then it is more reasonable to use only peak load values for determining G_f. Besides, they are easier to measure.

In light of Fig. 6, there seems to be still another source of error. From this figure it is apparent that the use of a single size specimen with different crack lengths cannot, due to inevitable random scatter, give information on the complete R-curve, or the complete size-effect curve. It pertains only to a portion of the curve, and does not indicate unambiguously the limiting value of the R-curve, which represents G_f (Fig. 6). If tests on single size specimens (without crack length measurements) do not give sufficient data on the R-curve, how can they unambiguously yield the R-curve asymptote?

R-Curves for Different Specimen Shapes.—The crack band model makes it possible to illustrate how much error is introduced when the R-curve determined for one specimen shape is used for another specimen shape. Calculations of R-curves for different geometries have been made using the same crack band parameters, see Fig. 8. The differences

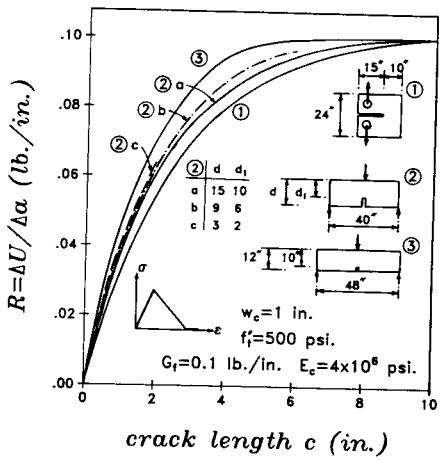

FIG. 8.—R-Curves Calculated by Crack Band Model for Same Material Parameters and Different Specimens

between some of these curves may seem large, however, they are not large compared to the inevitable statistical scatter of measured R-curve values. Therefore, the hypothesis of a unique R-curve appears to be acceptable for crude structural analysis, within a certain range of geometries. There exist, though, geometries for which a substantially different R-curve must be used (e.g., double-edge-cracked strip in tension versus eccentric compression).

Identification of Crack Band Model Parameters

The size effect law (Eq. 1) may be also exploited to identify the material parameters for the finite element crack band model (3,10). In this model the fracture energy is equal to the area under the tensile uniaxial stress-strain diagram in Fig. 7(*a*), times the effective width of the cracking front, w_c. Assuming this diagram to be bilinear, with elastic modulus E and mean strain-softening modulus E_t (<0), we have $G_f = f_t'^2\,(1 - E/E_t)w_c/2E$ from Ref. 9. Approximately, $w_c = 3d_a$ where d_a = maximum aggregate size (10).

For geometrically similar specimens, the finite element solution of the nominal stress at failure σ_N should depend only on the material parameters. There are four of them: f_t', E, G_f, and w_c. Parameter E_t is not independent since it is related to G_f. Consequently, for geometrically similar specimens, $P/bd = \sigma_N = \phi_1(f_t', E, G_f, w_c)$ in which ϕ_1 is a certain function. Now, according to Buckingham's II-theorem of dimensional analysis (1), the number n_s of independent nondimensional governing parameters should be $n_p - n_d$ where $n_p = 4$ = number of governing parameters and $n_d = 2$ = number of independent dimensions in these parameters (length and force). Thus, $n_s = 4 - 2 = 2$. So there can be only two independent nondimensional governing parameters. Along with the nondimensionalized function σ_N, they may be introduced as

$$s = \frac{\sigma_N}{f_t'}; \quad \theta = \frac{d}{w_c}; \quad \kappa = \frac{EG_f}{w_c f_t'^2} \qquad (14)$$

and function ϕ_1 reduces to

$$s = \phi_1(\theta, \kappa) \qquad (15)$$

Eqs. 14–15, describing the similitude of blunt fracture, greatly reduce the number of cases that have to be solved by finite elements in order to cover all possible situations.

For identifying the material of the crack band model, the following approach may be adopted. We choose a certain specimen geometry, and by testing specimens of different sizes we determine, by linear regression, parameters B and d_0 of the size effect law (Eq. 1). Then, by carrying out finite element solutions for geometrically similar specimens of different sizes, we determine the size effect plot as a function of the governing parameters θ and κ (Eq. 15). Finally, we determine the values of B and λ_0 for which Eq. 1 gives the optimum fit of this plot. The interjection of the size effect law not only facilitates analysis, but also has the advantage of smoothing and extending randomly scattered measured data. The detailed procedure is as follows:

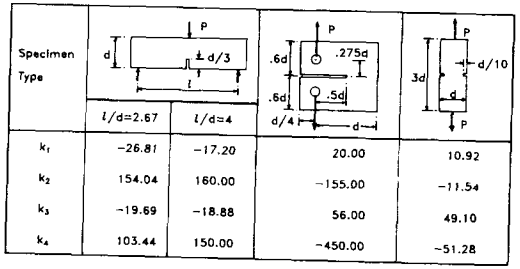

Specimen Type	$l/d=2.67$	$l/d=4$		
k_1	−26.81	−17.20	20.00	10.92
k_2	154.04	160.00	−155.00	−11.54
k_3	−19.69	−18.88	56.00	49.10
k_4	103.44	150.00	−450.00	−51.28

FIG. 9.—Coefficients for Determining Crack Band Model Parameters

1. Set $w_c = E = f_t' = b = 1$, and fix the value of κ ($\kappa = G_f$).
2. Fix the value of θ ($\theta = d$) and solve by a finite element program with incremental loading the maximum load P (the load-point displacements are prescribed and P is calculated as the reaction). Then calculate $s = P/\theta$.
3. Repeat step 2 for various θ values and construct the plot of s^{-2} versus θ.
4. Now, according to the size effect law in Eq. 1, this plot should ideally agree with $s = B[1 + (\theta/r)]^{-1/2}$, which is equivalent to $y = Ax + C'$ where $x = \theta$; $y = s^{-2}$; $A = (B^2 r)^{-1}$; $C' = B^{-2}$; and $r = d_0/w_c$. Determine the regression line of this plot; its y-intercept is C', from which $B = 1/\sqrt{C'}$, and its slope is A, from which $r = C'/A$. These values of B and r correspond to the previously fixed value of κ.
5. Repeat steps 1–4 for various values of κ and construct the graphs $B(\kappa)$ and $r(\kappa)$.

The numerical results show that the graphs of $B(\kappa)$ and $r(\kappa)$ are linear. Thus, calculation of only two points on each graph is sufficient, and the values may generally be expressed as $\kappa = k_1 + k_2 B$, and $r = k_3 + k_4 B$. Fig. 9 shows the calculation results for several typical fracture specimens.

As an example, consider again the data from Eq. 7. The test results are plotted as $1/\sigma_N^2$ versus d [Fig. 1(*b*)], and from the slope and the intercept of the regression line we get the values of B and d_0 (Eq. 1) as measured. For the data in Fig. 1(*b*) we have $B = 0.1817$ and $d_0 = 7.834$. Then, for this value of B, and using the values from Fig. 9, we get $\kappa = 11.9$ and $r = 8.4$. From this we finally obtain

$$w_c = \frac{d_0}{r}; \quad G_f = \frac{w_c}{E} f_t'^2 \kappa; \quad E_t = \left(\frac{1}{E} - \frac{2G_f}{w_c f_t'^2}\right)^{-1} \qquad \text{(16)}$$

Exploiting the size effect law (Eq. 1) makes it possible to do with a lesser amount of measurements. If the maximum load values for only a few specimens are fitted directly with the finite element program for the crack band theory, the values of material parameters which give good fits of data are quite ambiguous; even very different material parameter values yield equally good fits. This ambiguity and uncertainty is removed by the size effect law, which has the effect of smoothing and extrapolating the measured data.

Nonlinear finite element solution is not needed if equivalent linear fracture analysis is used. The value of G_f may then be calculated from Eq. 6 on the basis of the slope of the size effect regression plot and the value of $g(\alpha_0)$ obtained by an analytical or finite element solution according to linear elastic fracture mechanics.

In the preceding procedure based on Eq. 16, the value of w_c has been considered as unknown. As a rough approximation, however, $w_c \simeq 3d_a$ where d_a = maximum aggregate size (9). If this approximation is adopted, and if f_t' is known, then G_f is simply obtained from Eq. 16 on the basis of the slope of the regression plot for the size effect [Fig. 1(*b*)], and E_t is then evaluated from Eq. 16.

Identification of Nonlinear Fracture Models with Stress-Displacement Relation

Through a simple extension of the foregoing analysis, it is possible to determine the material parameters for Hillerborg's (12,17) and other nonlinear fracture models, in which a sharp crack is assumed and a relation between the relative displacement δ and normal stress σ across the line is introduced as a material property. The displacement δ lumps into a line the normal strain due to cracking accumulated over length w_c, and so

$$\delta(\sigma) = w_c \left[\epsilon(\sigma) - \frac{\sigma}{E}\right] \qquad \text{(17)}$$

where $\epsilon(\sigma)$ describes the tensile stress-strain diagram for the equivalent crack band model. Most simply, the σ-δ relation may be considered as a straight line of negative slope C_f [Fig. 7(*c*)], described as $\delta(\sigma) = (f_t' - \sigma)/C_f$ if $\sigma \geq 0$ and $\delta \geq 0$, but $\sigma = 0$ if $\delta \geq f_t'/C_f$. Equating the total relative displacement across the crack band according to both models and assuming the stress at the crack front (in a thin plate) to be approximately uniaxial, we have the relation $w_c\sigma/E + (f_t' - \sigma)/C_f = w_c[f_t'/E - (f_t' - \sigma)/E_t]$. This relation is satisfied for any σ if

$$\frac{1}{C_f} = w_c\left(\frac{1}{E} - \frac{1}{E_t}\right) \qquad \text{(18)}$$

Alternatively, we may use the condition of equal fracture energy for both theories; $G_f = f_t'^2/2C_f = w_c(E^{-1} - E_t^{-1}) f_t'^2/2$. From this, Eq. 18 results again.

Use of Generalized Size Effect Law

Eq. 1 is the simplest possible approximation to the size effect for blunt fracture. The most general size effect law may be stated in the form of the symptotic expansion: $\sigma_N = Bf_t'(a_0\eta^{-1} + 1 + a_1\eta + a_2\eta^2 + a_3\eta^3 + \ldots)^{-1/2r}$ where $\eta = (d/d_a)^r$ and f_t', B, r, a_0, a_1, a_2, ... are material parameters (6). The first order approximation obtained by setting $a_1 = a_2 = a_3 = \ldots = 0$, i.e.,

$$\sigma_N = Bf_t'\left[1 + \left(\frac{d}{d_0}\right)^r\right]^{-1/2r} \qquad \text{(19)}$$

is considerably more flexible than Eq. 1 for describing various possible shapes of the curve of log σ_N versus log d which may be obtained by finite element calculations (2). However, the size range of the available test data does not suffice for unambiguous determination of r.

If sufficiently broad data were available, then Eq. 19 could also be used to determine fracture parameters. Eq. 19 may be written as $Y = AX + C$ in which $X = d^r$, $Y = \sigma_N^{-2r}$, $A = C(\lambda_0 d_a)^{-r}$ and $C = (Bf_t')^{-2r}$. A set of r-values, e.g., 1, 0.8, 0.6, 0.4, may be chosen and, for each, one calculates by linear regression the values of A, C and the sum of squared deviations from the test data. One considers the dependence of this sum on r and identifies the r-value that minimizes this sum. Then $B = C^{-1/2r} f_t'$, $\lambda_0 = (CA)^{1/r}/d_0$. For $d/d_0 \to \infty$, we have the relation $\sigma_N^2 = B^2 f_t'^2 \, d_0/d = G_f E_c/g(\alpha_0)d$, from which we get for G_f again Eq. 6. The G_f values obtained for various r are rather different; however, within a not too broad range of sizes for which the tests were made, the predictions of fracture behavior are quite close to each other.

Conclusions

1. The size effect law of blunt fracture (Eq. 1) is useful for identifying the material parameters for nonlinear fracture, regardless of whether the R-curve approach, or the strain-softening crack band model, or the stress-displacement relation (Hillerborg's model) is used. The basic idea is to transform the size effect law to a linear plot and determine in this plot the regression line for the measured data obtained by tests of geometrically similar specimens of different sizes. The slope of this regression line then yields the fracture energy (the value of which is, by definition, size-independent), and the y-intercept yields the strain-softening modulus. The method can also be extended to certain dissimilar specimens of similar cross sections. The size effect law, the parameters of the crack band model, and the R-curve parameters are uniquely related. If one of them is specified, the others follow.
2. Exploiting the size effect law has four advantages:
   a. Statistically scattered measurements are smoothed [Fig. 1(*b*)].
   b. The range of the test data is extended, thus reducing ambiguity of data fitting and uncertainty in the material parameter values. Consequently, the experimentalist can get by with fewer tests covering a narrower range.
   c. Determination of R-curve as an envelope is made possible, while without the smoothing by the size effect law no envelope exists.
   d. A simpler measurement procedure than with the existing methods becomes possible. Only maximum load values are needed. They can be obtained even in a laboratory with the most rudimentary equipment. There is no need to measure the crack length, which avoids the ambiguity in defining and observing the location of the crack tip. No measurement of unloading or reloading compliance is needed.
3. When nonlinear fracture mechanics is applied for the purpose of determining the maximum load for monotonic loading, rather than the maximum load after a series of previous unloadings, it is more realistic to use only maximum loads also for the experimental calibration of the mathematical model.
4. Measuring maximum loads of specimens that have notches of various lengths but are of the same size does not provide sufficient basis for determining the nonlinear fracture properties, e.g., the R-curve.

Acknowledgment

Partial financial support under AFOSR Grant No. 830009 to Northwestern Univ. is gratefully acknowledged. Mary Hill deserves thanks for her dedicated secretarial assistance.

Appendix.—References

1. Barenblatt, G. I., "Similarity, Self-Similarity and Intermediate Asymptotics," Consultants Bureau, New York, NY, 1979 (translated from Russian).
2. Bažant, Z. P., "Comment on Hillerborg's Comparison of Size Effect Law and Fictitious Crack Model," Dei Poli Anniversary Volume, L. Cedolin, Ed., Politecnico di Milano, Milano, Italy, Oct., 1985.
3. Bažant, Z. P., "Crack Band Model for Fracture of Geomaterials," *Proceedings of the 4th International Conference on Numerical Methods in Geomechanics*, held in Edmonton, AB, Canada, June, 1982, Z. Eisenstein, Ed., Vol. 3.
4. Bažant, Z. P., "Fracture in Concrete and Reinforced Concrete," *Mechanics of Geomaterials: Rocks, Concretes, Soils*, Z. P. Bažant, Ed., John Wiley & Sons, Chichester, NY, 1985, pp. 259–304 (Proc. of IUTAM W. Prager Symposium held at Northwestern Univ., Sept., 1983).
5. Bažant, Z. P., "Size Effect in Blunt Fracture: Concrete, Rock, Metal," *Journal of Engineering Mechanics*, ASCE, Vol. 110, 1984, pp. 518–535.
6. Bažant, Z. P., "Fracture Mechanics and Strain-Softening of Concrete (Preprints)," *U.S.-Japan Seminar on Finite Element Analysis of Reinforced Concrete Structures*, Japan Society for the Promotion of Science, Tokyo, May, 1985, pp. 71–92.
7. Bažant, Z. P., and Cedolin, L., "Approximate Linear Analysis of Concrete Fracture by R-Curves," *Journal of Structural Engineering*, ASCE, Vol. 110, 1984, pp. 1336–1355.
8. Bažant, Z. P., and Estenssoro, L. F., "Surface Singularity and Crack Propagation," *International Journal of Solids and Structures*, Vol. 15, 1979, pp. 405–426, and Vol. 16, 1980, pp. 479–481.
9. Bažant, Z. P., and Kim, J. K., "Size Effect in Shear Failure of Longitudinally Reinforced Beams," *American Concrete Institute Journal*, Vol. 81, No. 5, 1984, pp. 456–468.
10. Bažant, Z. P., and Oh, B. H., "Crack Band Theory for Fracture of Concrete," *Materiaux et Constructions* (Materials and Structures), RILEM, Paris, Vol. 16, 1983, pp. 155–117.
11. Bažant, Z. P., and Oh, B. H., "Rock Fracture via Strain-Softening Finite Elements," *Journal of Engineering Mechanics*, ASCE, Vol. 110, No. 7, July, 1984, pp. 1015–1035.
12. Broek, D., *Elementary Engineering Fracture Mechanics*, Noordhoff International Publishing, Leyden, The Netherlands, 1974.
13. Hillerborg, A., Modéer, M., and Petersson, P. E., "Analysis of Crack Formation and Crack Growth in Concrete by Means of Fracture Mechanics and Finite Elements," *Cement and Concrete Research*, Vol. 6, 1976, pp. 773–782.
14. Irwin, G. R., "Fracture Testing of High Strength Sheet Material," (Report of a Special Committee), *ASTM Bulletin*, Jan., 1960, p. 29; (also Irwin, G. R., "Fracture Testing of High Strength Sheet Materials under Conditions Appropriate for Stress Analysis," *Report No. 5486*, Naval Research Laboratory, July, 1960).

15. Jenq, Y. S., and Shah, S. P., "Nonlinear Fracture Parameters for Cement Based Concrete: Theory and Experiments (Preprints)," *Applications of Fracture Mechanics to Cementitious Composites* (NATO Advanced Research Workshop), S. P. Shah, Ed., Northwestern Univ., Evanston, IL, Sept., 1984, pp. 213–253.
16. Krafft, J. M., Sullivan, A. M., and Boyle, R. W., "Effect of Dimensions on Fast Fracture Instability of Notched Sheets," *Cranfield Symposium 1961*, Vol. 1, pp. 8–28.
17. Mai, Y. W., "Fracture Measurements of Cementitious Composites (Preprints)," *Applications of Fracture Mechanics to Cementitious Composites* (NATO Advanced Research Workshop), S. P. Shah, Ed., Northwestern Univ., Evanston, IL, Sept., 1984, pp. 289–319.
18. Petersson, P. C., "Crack Growth and Development of Fracture Zones in Plain Concrete and Similar Materials," thesis presented to the Lund Institute of Technology, at Lund, Sweden, in 1981, in partial fulfillment of the requirements for the degree of Doctor of Philosophy.
19. Tada, H., Paris, P. C., and Irwin, G. R., *The Stress Analysis of Cracks Handbook*, Del Research Corp., Hellertown, PA, 1973.
20. Tattersall, H. G., Tappin, G., "The Work of Fracture and Its Measurement in Metals, Ceramics and Other Materials," *Journal of Materials Science*, Vol. 1, 1966, pp. 296–301.
21. Velazco, G., Visalvanich, K., and Shah, S. P., "Fracture Behavior and Analysis of Fiber Reinforced Concrete Beams," *Cement and Concrete Research*, Vol. 110, 1980, pp. 41–51.
22. Wecharatana, M., and Shah, S. P., "Slow Crack Growth in Cement Composites," *Journal of the Structural Division*, ASCE, Vol. 108, June, 1982, pp. 1400–1413.
23. Wittmann, F. H., Ed., "Fracture Mechanics of Concrete," Elsevier, The Netherlands, 1983, p. 680.